

Sinusoidally modulated $\text{ZnSe}_x\text{Te}_{1-x}$ superlattices: Fabrication and structural studies

P. M. Reimer* and John R. Buschert

Turner Precision X-ray Laboratory, Goshen College, Goshen, Indiana 46526

S. Lee and J. K. Furdyna

Physics Department, University of Notre Dame, Notre Dame, Indiana 46556

(Received 13 July 1999; revised manuscript received 8 November 1999)

Semiconductor “sinusoidal superlattices” of $\text{ZnSe}_x\text{Te}_{1-x}$ —that is, periodic structures in which the chemical composition parametrized by x varies sinusoidally along one direction—were fabricated by rotating a substrate through an inhomogeneous distribution of constituent fluxes within a molecular beam epitaxy growth chamber. The modulation of chemical composition x is accompanied by modulation of strain, owing to the difference in Zn-Se and Zn-Te bond lengths. By fitting x-ray diffraction scans around the (002), (004), and (006) Bragg reflections for (001)-oriented $\text{ZnSe}_x\text{Te}_{1-x}$ sinusoidal superlattices to a simple scattering theory, we have determined both the strain and the chemical modulation amplitudes in these structures.

I. INTRODUCTION

We describe the fabrication and structure of semiconductor “sinusoidal superlattices,” i.e., periodic structures in which the composition of a semiconductor alloy varies sinusoidally (or very nearly so) in one direction. We will concentrate on the system $\text{ZnSe}_x\text{Te}_{1-x}$ with sinusoidally modulated x , about which our knowledge is the most advanced. In an earlier paper¹ some of the present authors had already noted that this II-VI ternary system could be prepared as a periodic structure that shows only one set of x-ray superlattice satellite reflections, indicating just one Fourier component of compositional modulation. In that paper the authors had mistakenly assumed the origin of the modulation to be spontaneous, arising from the nature of growth dynamics in the presence of surface steps. We have since been able to link the formation of this modulation to the rotation of the substrate during molecular beam epitaxy (MBE) growth in the presence of an uneven distribution of constituent fluxes (Te and Se in the present case). This understanding offers a means by which to fabricate such sinusoidally modulated structures with controlled period and modulation amplitude.

An x-ray θ - 2θ scan of a typical compositionally modulated $\text{ZnSe}_x\text{Te}_{1-x}$ structure is shown in Fig. 1. In a qualitative sense, x-ray diffraction depicts the square of the Fourier transform of electron density in a sample. X-ray diffraction scans from semiconductor superlattices with abrupt interfaces typically have *many* satellite peaks around each Bragg reflection,^{2,3} corresponding to the many Fourier components that add up to form a square-wave composition profile. The fact that Fig. 1 shows just *one* peak on either side of each fundamental Bragg peak implies the existence of only one Fourier component in the compositional modulation of this system—hence the term “sinusoidal” superlattices. We show below that such superlattice peaks can arise from either a purely chemical modulation of the sample, or a pure modulation of the lattice parameter, or—as is much more likely—a combination of the two. We elaborate a simple scattering theory that allows composition and strain modulation amplitudes to be separately and quantitatively determined.

Superlattices with a sinusoidal compositional profile are

unusual in several respects: to achieve such a profile by conventional growth methods (e.g., by some form of continuous shutter programming), would be simply unrealistic. Such a profile in turn results in a band structure, that leads to novel optical properties via relaxation of the “standard” selection rules.⁴ Furthermore, one can grow “massive” superlattices, of multimicrometer thicknesses and with many hundreds of periods without any wear on the shutters. A superlattice of this type is thus an anisotropic medium in its own right, even when the period is too short to achieve charge carrier confinement.

II. FABRICATION OF SINUSOIDAL SUPERLATTICES

The $\text{ZnSe}_x\text{Te}_{1-x}$ superlattices were fabricated using a Riber 32 R&D molecular beam epitaxy (MBE) machine equipped with elemental Zn, Se, and Te sources. The superlattices were grown on (100) GaAs substrates mounted with indium on a molybdenum sample mounting block with a diameter of 5.6 cm. After being placed in the preparation

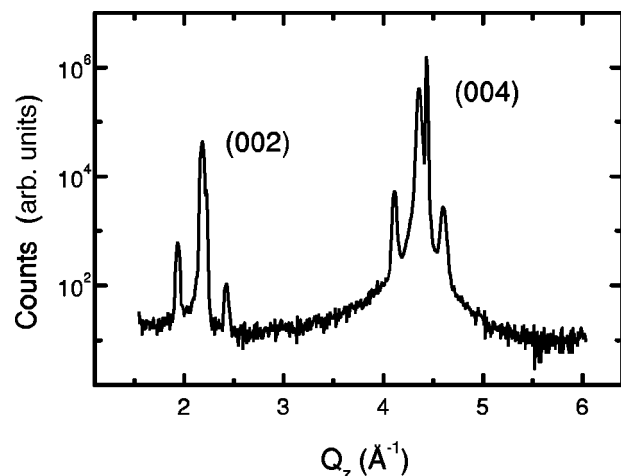


FIG. 1. A typical x-ray scan, showing superlattice satellites for (002) and (004) Bragg peaks. The most intense, narrow peak in the (004) group is the GaAs substrate (004) Bragg peak.

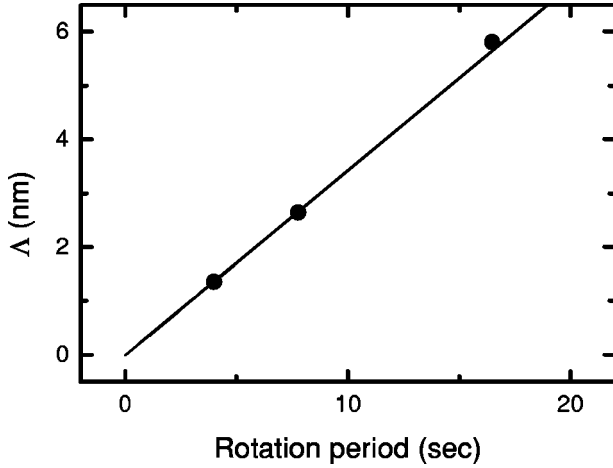


FIG. 2. Plot of superlattice period Λ as a function of the period of rotation rate.

chamber, the GaAs substrates were cleaned *in situ* by oxide desorption, by heating to 600 °C. The completion of the cleaning process was recognized by monitoring the reflection high-energy electron diffraction pattern. Cleaned GaAs substrates were then cooled to the superlattice growth temperature (ca. 300 °C). The Se and Te evaporation cells were placed on opposite sides of the mounting block, each approximately 12 cm away from the mounting block. This configuration yields a nonuniform flux distribution across the mounting block (Se rich on one side, Te rich on the other).

The rotation of the mounting block about an axis approximately perpendicular to the substrate surface thus makes the substrate pass regularly through different flux distribution areas, resulting in alternating Se-rich and Te-rich layers. We prepared three superlattices under identical growth conditions, varying only the rate at which the substrate was rotated in the chamber. We then made radial (θ - 2θ) x-ray scans of the samples after they were taken out of the growth chamber. The separation in reciprocal space ΔQ between the superlattice peaks is inversely proportional to the superlattice modulation distance Λ , i.e., the superlattice period. In Fig. 2, we plot the superlattice period Λ as a function of the period of rotation T used in fabricating the respective specimens. It is very clear that the superlattice period Λ is directly proportional to the period of rotation T : the faster the sample is rotated, the shorter is the repeat distance of the superlattice modulation. In other studies (not shown) we found the amplitude of the superlattice peaks increasing as the distance between the sample and the center of rotation of the mounting block was increased.

III. STRUCTURAL ANALYSIS: CHEMICAL AND STRAIN MODULATION

It has already been shown in the Introduction that the x-ray diffraction data from the $\text{ZnSe}_x\text{Te}_{1-x}$ superlattices under consideration imply a sinusoidal modulation of the chemical composition parameter x . We can usefully approximate this composition profile as varying with depth z about a mean value x_0 in the form

$$x(z) = x_0 + \frac{M}{2} \cos\left(\frac{2\pi z}{\Lambda}\right), \quad (1)$$

where $x(z)$ is the atomic fraction of Se at depth z , M is the *modulation amplitude* of the composition (a number less than 1), and Λ is the superlattice period.

The consequences of the approximation in Eq. (1) on x-ray diffraction are developed in the Appendix. In particular, the following expression [Eq. (A9)] gives the intensities of the two satellite peaks associated with a given fundamental x-ray Bragg reflection in such a sinusoidally modulated system:

$$I_{\pm} = \left(\frac{b_0}{2}\right)^2 \left[\eta_{\mp} \epsilon \left(\frac{m\Lambda}{d_0} \pm 1 \right) \right]^2, \quad (2)$$

where the upper and lower subscripts refer to the high- and low-angle satellites, respectively; $\eta(M)$ is proportional to M [see Eq. (A6)], the amplitude of chemical modulation; ϵ is the amplitude of strain modulation; m is the order of the fundamental reflection [$m=2$ for satellites associated with the (002) Bragg reflection, $m=4$ corresponds to (004), etc.]; and b_0^2 is the intensity of the fundamental Bragg reflection (in our case, the intensity of the central $\text{ZnSe}_x\text{Te}_{1-x}$ peak). The dependence on the order m is clearly seen in Fig. 1 in the form of the different asymmetries of I_+ and I_- for $m=2$ and $m=4$.

One might suppose that two measurements, say I_+ and I_- near *one* Bragg reflection, would be sufficient to determine the two unknowns η and ϵ in Eq. (2). Since Eq. (2) really represents *two* equations, we can eliminate one unknown (say, η) between them. However, this results in an expression which is biquadratic in ϵ .

Thus, to establish the values of ϵ and η unambiguously it is necessary to make observations near at least *two* Bragg orders. In fact, in this paper we will use satellite data near *three* Bragg orders (thus overdetermining the two model parameters), and then vary ϵ and η to find the best fit.

A. Experimental considerations

In practice, we set out to measure the *integrated intensities* of low- and high-angle satellites and fundamentals at three Bragg reflections, as this is notoriously more reliable to measure than amplitudes alone, and is entirely equivalent when the peak shapes being compared are the same (see below). The θ - 2θ x-ray scans used in this analysis were obtained on an x-ray diffractometer fitted with a Si(111) monochromator in double-axis mode (that is, without an analyzer crystal).

The samples which we investigated were grown on substrates with a considerable ($>3^\circ$) miscut relative to the (100) plane. This results in satellite peaks which are not collinear with the fundamental Bragg peaks in reciprocal space, so care must be taken that the full integrated intensity of the satellites is measured. To ascertain that this is the case, we oriented each sample on the diffractometer such that the satellite peaks lay in the plane of diffraction, and relaxed the detector collimation. After making a θ - 2θ scan, we rocked 2θ at the satellite-peak positions, to make sure that collimation had been sufficiently relaxed to capture the full peak intensity.

The analysis of experimental data in terms of Eq. (2) was carried out as follows. Using the Levenburg-Marquardt fit-

ting algorithm,⁵ we fitted the data from each Bragg order to a three-peak combination—the fundamental $\text{ZnSe}_x\text{Te}_{1-x}$ reflection and the two satellites. Peak shape (pseudo-Voigtian) parameters, such as the peak width, were allowed to vary, but all three peaks were constrained to have the same peak shape. Only the amplitudes and relative peak positions (parametrized by Λ) were allowed to differ among the three peaks. In fact, the peak shapes and widths of the fundamental and of the satellites do appear identical—indicating that the superlattice modulation coherence length is comparable to the atomic coherence length.

The resulting peak intensities were corrected for the gradual variations in the b_0 and η factors as a result of the variation of the atomic scattering factors, f_{Zn} , f_{Se} , and f_{Te} as a function of q ,⁶ as well as for Lorentz polarization effects,⁷ and sample geometry effects. Best-fit values for the chemical and strain amplitude were extracted by taking weighted averages of the parameters found from fits at each Bragg order. Experimental uncertainty was estimated by varying individual model peak intensities to increase the χ^2 fitting criteria a constant amount, and recalculating ϵ and η . A typical fit to the x-ray data obtained for one of the superlattices ($\Lambda = 46.33 \text{ \AA}$) is shown in Fig. 3.

B. Results: Modulation amplitudes

We list the results of our fitting analysis for two superlattices in Table I, which includes the sample fit shown in Fig. 3. The intensities of all six satellite peaks were determined by the same *two* free fitting parameters ϵ and M for each of the superlattices. No other fitting parameters were used in the analysis. The agreement of the fit and the data provide encouraging confirmation of the general outlines of the scattering theory put forth in the Appendix.

The parameters obtained from the fit (see Table I) may be interpreted as follows. Considering sample 2 for purposes of illustration, the anion layers in this superlattice consist on average of 63% Se, 37% Te. $M = 0.157$ obtained from the fit indicates that the Se concentration varies sinusoidally between 55% and 71%, i.e., $\pm 8\%$ around the mean value of 63%. The distance between the peak Se concentrations (i.e., the superlattice period) is 46.33 \AA . It is apparent that the deposition techniques described in this report are leading to *significant* modulation amplitudes, of the order of the mean Se concentration itself.

Several ‘‘reality checks’’ may be made on the parameters. From the table we note, for example, that ϵ has the opposite sign from M . This indeed makes sense: a depth z where the cosine function is positive in Eq. (A1) corresponds to a higher than average concentration of Se. At the same depth z we would expect the lattice parameter in Eq. (A7) to be less than its average value, since $a_{\text{ZnSe}} < a_{\text{ZnTe}}$. A second check on the parameters is as follows: ϵ is the fractional strain amplitude relative to the mean lattice parameter. Without going to the trouble of making an exact elastic calculation, we can say that the strain amplitude, when expressed as a fraction of the difference ($a_{\text{ZnSe}} - a_{\text{ZnTe}}$), is likely to be of the same order of magnitude as the chemical modulation fraction M , which is already relative to the difference of chemical concentrations. The last two columns in Table I show that this is indeed the case. The larger uncertainty in M

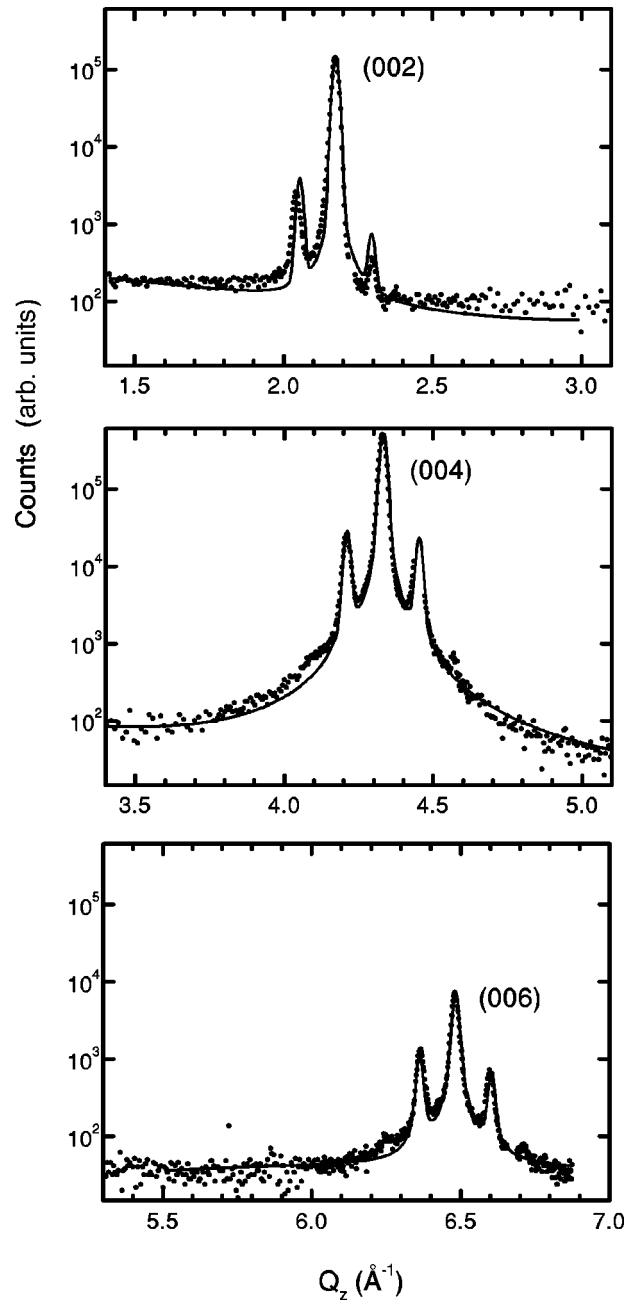


FIG. 3. θ - 2θ scans for sample 2 in Table I near (top to bottom) the (002), (004), and (006) Bragg reflections. For the fit, points corresponding to GaAs substrate reflections were excised. This made it particularly hard to fit accurately the high-angle satellite near (004).

for the first sample arises because the GaAs substrate reflection (excised from the data in the fitting process in Fig. 3) falls on top of the (004) $s = +1$ satellite, making its amplitude difficult to determine.

The satellite intensities do not change monotonically with reflection order, but instead vary rather widely from one order to the next, both relative to the fundamental as well as relative to each other. The theory accounts for this variation. In general terms, it may be seen from the m dependence of Eq. (2) that when $m\epsilon$ is of order a/Λ , drastic cancellations can take place. Nor is it likely that any two satellites would have the same intensity, unless either $M = 0$ or $\eta = 0$, and

TABLE I. Parameters found from the fitting procedure described in the text for two $\text{ZnSe}_x\text{Te}_{1-x}$ samples. a_0 is the mean lattice parameter; and x_0 is the mean Se fraction implied by a_0 ; Λ is the period of superlattice modulation; ϵ is the fractional strain modulation amplitude; and M is the chemical modulation amplitude.

Sample	a_0	x_0	Λ	ϵ	$\frac{\epsilon a_0}{a_{\text{ZnSe}} - a_{\text{ZnTe}}}$	M
1	5.804 Å	0.682	52.00 Å	-0.0124 ± 0.002	0.167	0.108 ± 0.04
2	5.826 Å	0.631	46.33 Å	-0.0139 ± 0.002	0.187	0.157 ± 0.01

this would be rather unphysical in alloys involving lattice-mismatched constituents, as in the case of $\text{ZnSe}_x\text{Te}_{1-x}$ considered here.

Finally, we have observed hints of higher-order satellite peaks in some of the samples, particularly among the (006) order peaks, as can be seen by close inspection of Fig. 3. This indicates the samples are not *exactly* sinusoidal, having small Fourier components of higher orders. However, the sinusoidal approximation which we have been using to model the scattering still turns out to be very useful, and able to capture and characterize some of the most important features of these new materials. It may also be seen from Eq. (2) that the m -containing term can eventually dominate the remaining terms, causing a general increase in relative superlattice satellite intensities as the reflection order increases. This trend is clearly seen in our data (see Fig. 3). Indeed, according to a more complete theory that takes into account higher-order Fourier components (not shown in this paper), it would also be expected that the higher-order satellites would increase relative to the fundamental at higher-order Bragg reflections.

Finally, we note that the misalignment of the superlattice modulation with the crystallographic directions is not taken into account in the scattering theory. This—and perhaps to a minor degree geometrical factors—probably account for most of the discrepancies between our fits and the diffraction data.

IV. CONCLUDING REMARKS

We have demonstrated that $\text{ZnSe}_x\text{Te}_{1-x}$ superlattices with a sinusoidal modulation of composition x can be fabricated by MBE by rotating the substrate in the presence of an inhomogeneous distribution of the anion flux over the substrate area. We then measured quantitatively the strain and composition modulation amplitudes. It is clear from this that both the superlattice period and amplitude can be continuously controlled with this “shutterless” approach to the growth of modulated structures, simply by programming the rotation speed within the rotation cycle, and choosing the position of the sample relative to the center of rotation. The quality of the superlattices is very high, as judged by the criterion that the satellite peaks are as narrow as the “parent” Bragg reflections.

Finally, the physics of the superlattice formation by rotation in uneven fluxes is so “obvious” as to appear trivial. The inhomogeneity of the anion fluxes was in the present case achieved by the Se and Te source configurations. It is therefore important to note that, using analogous *cation*

source configurations and similar rotation rates, so far we have not succeeded in forming superlattices in alloys with one anion and two cations (e.g., ZnCdSe or CdMnTe). Thus, if the sources are far enough apart and the rotation is sufficiently slow, it seems one should be able to form superlattices with any ternary combination of elements;⁸ however, it appears that the tendency to form a sinusoidal superlattice does depend on the different chemical species involved and their interactions.⁹

ACKNOWLEDGMENTS

The authors are grateful to A. Waag and W. Faschinger for valuable comments on the different behavior of Se and Te during MBE growth. This work was supported by the U.S. Department of Energy Grant No. 97ER45644.

APPENDIX: SCATTERING FROM A SINUSOIDAL SUPERLATTICE

We would like to analyze x-ray scattering expected from the lattice of an alloy in which the chemical composition is modulated sinusoidally along one direction (say, \hat{z}). This analysis is based on Guinier’s treatment¹⁰ of small amplitude strain and chemical waves, as used also by Miceli and Zabel.¹¹ Based on the observation of just a single order of superlattice reflections around each fundamental Bragg peak, we will assume that the chemical composition in our $\text{ZnSe}_x\text{Te}_{1-x}$ system can be expressed by x varying about a mean value x_0 as

$$x(z) = x_0 + \frac{M}{2} \cos\left(\frac{2\pi z}{\Lambda}\right), \quad (\text{A1})$$

where M is the modulation amplitude of the Se concentration, a number not greater than 1, and Λ is the modulation length (i.e., the superlattice period).

For scattering vectors $\mathbf{q} = q\hat{z}$, the scattering amplitude $A(q)$ may be calculated as if arising from a chain of atoms at discrete positions z_n with scattering amplitudes f_n from

$$\begin{aligned} A(q) &= \sum_n f_n e^{iqz_n} = \sum_r \left[\sum_j f_j e^{iqz_{jr}} \right] e^{iqz_r} \\ &\approx \sum_r \left[\sum_j f_j(z_r) e^{iqz_j} \right] e^{iqz_r}. \end{aligned} \quad (\text{A2})$$

The third expression is a rewriting of the sum as a summation over the j atoms within the repeating (unit) cell at relative positions u_j ; and then over all the r unit cells at posi-

tions z_r . The scattering intensity I is then proportional to $|A(q)|^2$ in the kinematic (weak scattering) approximation.

In the present case, the modulation direction $\hat{\mathbf{z}}$ is (almost) normal to the (00 l) planes of the zinc-blende lattice of $\text{ZnSe}_x\text{Te}_{1-x}$. With one side of the cubic unit cell having length a , cation and anion layers alternate at increments of distance of $a/4$ along $\hat{\mathbf{z}}$. So, $u_j = ja/4$, $f_2 = f_4 = f_{\text{Zn}}$, and taking into account Eq. (A1),

$$f_1 = f_3 = f_{\text{Te}} + x_0(f_{\text{Se}} - f_{\text{Te}}) + \frac{M}{2}(f_{\text{Se}} - f_{\text{Te}}) \cos\left(\frac{2\pi z}{\Lambda}\right). \quad (\text{A3})$$

The unit cell sum may then be cast in the form

$$\sum_{j=1}^4 f_j(z_r) e^{iqu_j} = b_0 \left[1 + \eta \cos\left(\frac{2\pi(z+a/4)}{\Lambda}\right) \right], \quad (\text{A4})$$

where, to zeroth order in q near the first three permitted reflections at (002), (004), and (006), we have

$$b_{0(002)} = -2[f_{\text{Te}} + x_0(f_{\text{Se}} - f_{\text{Te}}) - f_{\text{Zn}}] = b_{0(006)}, \quad (\text{A5})$$

$$b_{0(004)} = -2[f_{\text{Te}} + x_0(f_{\text{Se}} - f_{\text{Te}}) + f_{\text{Zn}}],$$

and

$$\eta = \frac{1}{b_0} \left\{ \frac{M}{2}(f_{\text{Se}} - f_{\text{Te}}) \sqrt{2 \left[1 + \cos\left(\frac{\pi a}{\Lambda}\right) \right]} \right\}. \quad (\text{A6})$$

Strain modulation

Above, the scattering power modulation was cast in the form $b_n = b_0[1 + \eta \cos(2\pi z\Lambda)]$. We now introduce a similar sinusoidal form for the *lattice positions*. The position z_r of unit cell r may be found by summing up the spacings a_k of all the previous unit cells. The mean value of the a_k is a . Because of modulation of the chemical species, we would also expect a modulation of the lattice spacing, which can be represented most generally with a Fourier sum:

$$z_r = \sum_{k=0}^r a_k = \sum_{k=0}^r a \left[1 + \sum_s \epsilon_s \cos\left(\frac{2\pi s}{\Lambda} z_k\right) \right] \\ \approx ra + \epsilon \frac{\Lambda}{2\pi} \sin\left(\frac{2\pi}{\Lambda} ra\right). \quad (\text{A7})$$

Since our experimental results only showed one set of satellites, we kept only the $s=1$ component $\epsilon_1 \equiv \epsilon$, and then approximated the resulting sum with an integral.

Substituting this expression for z_r into Eq. (A2), and developing the expressions further with ‘‘small angle’’ approximations valid for $\epsilon \ll 2\pi/\Lambda q$, we are left with terms which all contain lattice sums that approximate δ functions for large r . Let G be one of the reciprocal lattice vectors from the unstrained, unmodulated lattice, i.e., $G_m = 2\pi m/a$. Then the terms may be grouped as follows:

$$A(q) \approx b_0 \delta(q - G) + \left(\frac{b_0 \eta}{2} + \frac{b_0 q \epsilon}{2} \frac{\Lambda}{2\pi} \right) \delta\left(q + \frac{2\pi}{\Lambda} - G\right) \\ + \left(\frac{b_0 \eta}{2} - \frac{b_0 q \epsilon}{2} \frac{\Lambda}{2\pi} \right) \delta\left(q - \frac{2\pi}{\Lambda} - G\right). \quad (\text{A8})$$

It follows immediately that the intensity of the fundamental at $q=G$ is b_0^2 ; and that the intensities of the satellites at $q = G + 2\pi/\Lambda$ and $q = G - 2\pi/\Lambda$ are

$$A^2\left(G - \frac{2\pi}{\Lambda}\right) = \left(\frac{b_0}{2}\right)^2 \left[\eta + \left(G - \frac{2\pi}{\Lambda}\right) \epsilon \frac{\Lambda}{2\pi} \right]^2 \\ = \left(\frac{b_0}{2}\right)^2 \left[\eta + \epsilon \left(\frac{m\Lambda}{a} - 1\right) \right]^2; \quad (\text{A9}) \\ A^2\left(G + \frac{2\pi}{\Lambda}\right) = \left(\frac{b_0}{2}\right)^2 \left[\eta - \epsilon \left(\frac{m\Lambda}{a} + 1\right) \right]^2,$$

where m is the Bragg reflection order. These are the equations of central importance to the analysis of x-ray diffraction from sinusoidal superlattices, shown as Eq. (2) in the body of the article.

*Electronic address: paulmr@goshen.edu

¹S. P. Ahrenkiel, S. H. Xin, P. M. Reimer, J. J. Berry, H. Luo, S. Short, M. Bode, M. Al-Jassim, J. R. Buschert, and J. K. Furdyna, *Phys. Rev. Lett.* **75**, 1586 (1995).

²M. Korn, M. Li, S. Tiong-Palisoc, M. Rauch, and W. Faschinger, *Phys. Rev. B* **59**, 10 670 (1999).

³P. Yashar, M. R. Pillai, J. Mirecki-Millunchick, and S. A. Barnett, *J. Appl. Phys.* **83**, 2010 (1998).

⁴G. Yang, S. Lee, and J. K. Furdyna (unpublished). We also mention parenthetically that in optical experiments we have observed very bright photoluminescence (PL) from such sinusoidal $\text{ZnSe}_x\text{Te}_{1-x}$ superlattices. This was rather surprising, since modulated structures of this combination of materials are assumed to have a staggered (i.e., ‘‘type-II’’) band alignment, suggesting that optical transitions in this system should be indirect.

⁵W. H. Press, B. P. Flannery, S. A. Teukolsky, and W. T. Vetterling, *Numerical Recipes in C* (Cambridge University Press, Cambridge, 1988).

⁶J. A. Ibers and W. C. Hamilton, *Revised and Supplementary Tables*, *International Tables for X-ray Crystallography* Vol. IV

(Kynoch Press for the IUCr, Birmingham, 1974), p. 72.

⁷B. E. Warren, *X-ray Diffraction* (Addison-Wesley, Reading, MA, 1969).

⁸W. Fischinger and D. Hommel (private communication). Several researchers have informed us that they saw hints of modulation in MBE growth in the presence of stage rotation.

⁹S. Lee, F. Peiris, V. Bindley, and J. K. Furdyna, in *International Conference on Frontiers in Semiconductor Lasers and Quantum Dot Physics* (IAPS Press, La Jolla, CA, 1998). This reference demonstrates that even a small amount of Se tends to very effectively impede the incorporation of Te. Thus, although the rotation of the stage tends to trigger the growth described in this paper, issues such as the element-specific sticking coefficients and the difference in surface diffusion of Se and Te after they make contact with the surface are expected to be important in the process as well.

¹⁰A. Guinier, *X-ray Diffraction in Crystals, Imperfect Crystals, and Amorphous Bodies* (Freeman, San Francisco, 1963).

¹¹P. Miceli and H. Zabel, *Z. Phys. B: Condens. Matter* **74**, 457 (1989).